Producing Known Complex Modulation Signals for Calibration of Optical Modulation Analyzers

T. Dennis[1] and B. Nebendahl[2]
[1]*National Institute of Standards and Technology, 325 Broadway, Boulder, CO 80305*
[2]*Agilent Technologies, Digital &Photonic Test, Herrenberger Strasse 130, 71034 Böblingen, Germany*
tasshi@boulder.nist.gov

Abstract: A family of optical modulation signals with known properties was generated using three phase-locked lasers for calibration of the complex measurement plane. Patterns predicted from first principles were measured with a real-time optical modulation analyzer.
OCIS codes: (060.1660) Coherent communications; (060.4080) Modulation; (060.5060) Phase modulation; (120.3940) Metrology

1. Introduction

Coherent optical communications techniques with complex modulation formats have become the preferred method for achieving data rates of 100 Gb/s and beyond on a single optical carrier. Complex formats modulate both amplitude and phase to increase the spectral efficiency of a network by increasing the number of bits per transmitted symbol. To support these higher-order modulation formats, optical waveform metrology must be capable of measuring amplitude and phase at bandwidths much higher than the data rate itself [1]. This includes an accompanying need to be able to generate complex signals of known amplitude and phase. Waveform metrology is critical to the success of these new approaches because the signal margins are much tighter, whether viewed in terms of eye-pattern closure, optical signal-to-noise-ratio (OSNR), or error-vector-magnitude (EVM).

A variety of methods exist that are capable of characterizing both the magnitude and phase of complex modulated optical signals, including but not limited to quadrature detection with electrical sampling [1], linear optical sampling [2,3], non-linear optical sampling [4], and coherent spectrum analysis [1]. These methods are varied in that they may operate in the time or frequency domain, use real- or equivalent-time sampling, leverage linear or nonlinear optical phenomena, and have topologies that mimic or differ from the design of coherent network receivers.

Regardless of the methods and implementation, a technical challenge common to all of these metrology tools is obtaining an accurate calibration so that quantitative rather than qualitative results can be obtained. In addition to the well documented challenge of calibrating both the amplitude and time axes of digital communications analyzers (sampling oscilloscopes) [5], a complex modulation analyzer must also have a calibrated phase axis. Viewed differently, the in-phase and quadrature amplitude axes of the analyzer must be simultaneously well characterized. Ideally, the measurement of a signal that uniformly spans the complex plane, for example 64-QAM, will be measured accurately and displayed uniformly in both the in-phase and quadrature directions. Therefore, the time and frequency characteristics of the instrument, as well as the phase and amplitude, must be well known. Such instruments can rely heavily on software algorithms in order to present a signal in a meaningful way, by correcting for carrier phase drift, polarization multiplexing, and gain variations. In effect, such instrumentation acts like a golden receiver in the complex plane with a bandwidth that exceeds the signals to be measured.

Calibration of the complex measurement plane is difficult because the generation of modulated test signals is inherently complicated, and the devices used typically have an imperfect response. For example, the dual-parallel Mach-Zehnder modulator can generate an arbitrary complex signal; however, its amplitude response is not perfectly linear and the device must be operated at three independent bias points that are subject to drift. Such imperfections alone are not a problem if there is an independent way to verify the response, but therein lies the problem that the metrology tools designed for such measurements currently lack the necessary calibration or verification.

To circumvent the challenge of trying to correct for or independently characterize an imperfect device response, we developed a family of simple calibration test signals that can be derived from first principles. Our approach is based on a high-accuracy heterodyne technique for the calibration of high-speed photoreceivers [6], which, as demonstrated here is a simplistic form of arbitrary waveform generation using three sinusoidal tones. Three narrowband lasers were phase-locked to each other separated by known frequencies in the gigahertz range. Two of the lasers were combined to form a signal for measurement, while the third laser served as an external local oscillator (LO) for the instrumentation under test. The electric field of the signal E_s and the local oscillator E_{LO} can be written as

$$E_s(t) = E_1 e^{i(\omega_1 t+\theta_1)} + E_2 e^{i(\omega_2 t+\theta_2)} \quad (1)$$

$$E_{LO}(t) = E_{LO} e^{i(\omega_{LO} t+\theta_{LO})}, \quad (2)$$

where the subscripts 1, 2, and *LO* denote the three lasers each having amplitudes E, frequency ω, and phase θ. Demodulating E_s in a quadrature receiver with E_{LO} as the local oscillator, followed by square-law balanced detection, gives the in-phase (I) and quadrature (Q) voltage signals proportionally as

$$I(t) \propto E_s(t) \cdot E_{LO}(t)^* + E_s(t)^* \cdot E_{LO}(t) \quad (3)$$

$$Q(t) \propto E_s(t) \cdot E_{LO}(t)^* e^{-i\pi/2} + E_s(t)^* \cdot E_{LO}(t) e^{i\pi/2}. \quad (4)$$

More specifically in terms of the electric-field components of each laser we have,

$$I(t) \propto E_1 \cdot \cos((\omega_1 - \omega_{LO})t + \theta_1 - \theta_{LO}) + E_2 \cdot \cos((\omega_2 - \omega_{LO})t + \theta_2 - \theta_{LO}) \quad (5)$$

$$Q(t) \propto E_1 \cdot \sin((\omega_1 - \omega_{LO})t + \theta_1 - \theta_{LO}) + E_2 \cdot \sin((\omega_2 - \omega_{LO})t + \theta_2 - \theta_{LO}). \quad (6)$$

The shape of the modulation pattern in the complex plane described by $I(t)$ and $Q(t)$ is determined by the amplitude of E_1 relative to E_2, and the frequency differences between ω_1, ω_2, and ω_{LO}. If the three lasers are phase-locked to each other, the phase offsets θ_1, θ_2, and θ_{LO} are all constant with time and their values determine only the angular orientation of the modulation pattern, but not the shape.

The black solid line of Fig. 1 plots equations (5) and (6) in the complex plane with $E_1 = E_2$ at a difference frequency of $(\omega_1 - \omega_2)/2\pi = 5$ GHz. The LO laser was offset by 1 GHz from one of the signal lasers, as shown in Fig. 1. The 5:1 ratio between the difference frequencies results in a repeated modulation pattern with five lobes. The grey dotted line simulates the result of a coherent receiver with a 5 % gain imbalance of the quadrature (Q) photoreceiver. The distortion caused by the gain imbalance is significant and not simply radially symmetric.

2. Experimental setup

Figure 2 shows the experimental setup for generating the calibration test signal and the optical connections to the complex modulation analyzer. The two lasers that were combined to form the measurement signal are fiber lasers having linewidth specifications of < 1 kHz. The phase-locked-loop system that combines them applies feedback to a piezoelectric tuning element in one of the laser cavities as well as an external acousto-optic modulator for fast phase corrections. The third laser, which serves as an external LO for the modulation analyzer, is a semiconductor waveguide laser with a linewidth specification of 5 kHz. Feedback to this laser from a second phase-locked loop is provided by direct current modulation. The phase-lock systems use a double-heterodyne technique, as described in [6], to control the optical difference frequencies between the lasers by use of sinusoidal RF synthesizers. The synthesizer frequencies can be adjusted to change the difference frequencies between the lasers, which will result in different patterns generated in the complex plane. In all the measurements presented here, the difference frequency between fiber laser #2 and the LO laser was fixed at 1 GHz, whereas the frequency between fiber lasers #1 and #2 was varied. In addition, the optical power from the two fiber lasers was made equal to within 1 %, with a combined power of 650 μW. The LO laser had an optical power of about 8 mW.

The optical modulation analyzer (OMA) was a commercial instrument based on a polarization-diversity quadrature optical receiver with 40 GHz balanced detection. The electrical sampling of the detected signals was provided by a four-channel real-time oscilloscope with a 13 GHz bandwidth sampling at 40 GSa/s.

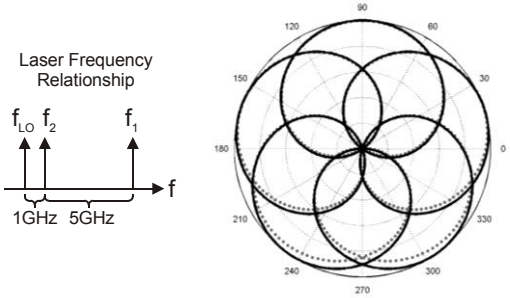

Fig. 1. Calculated modulation patterns for ideal quadrature receiver operation (black curve) and a 5 % receiver gain imbalance (grey dots).

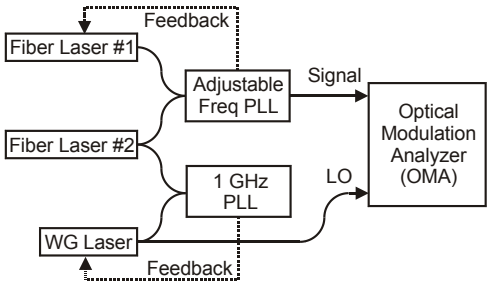

Fig. 2. The calibration signal generator, showing connections to a modulation analyzer. PLL: phase-locked loop; WG: waveguide; LO: local oscillator.

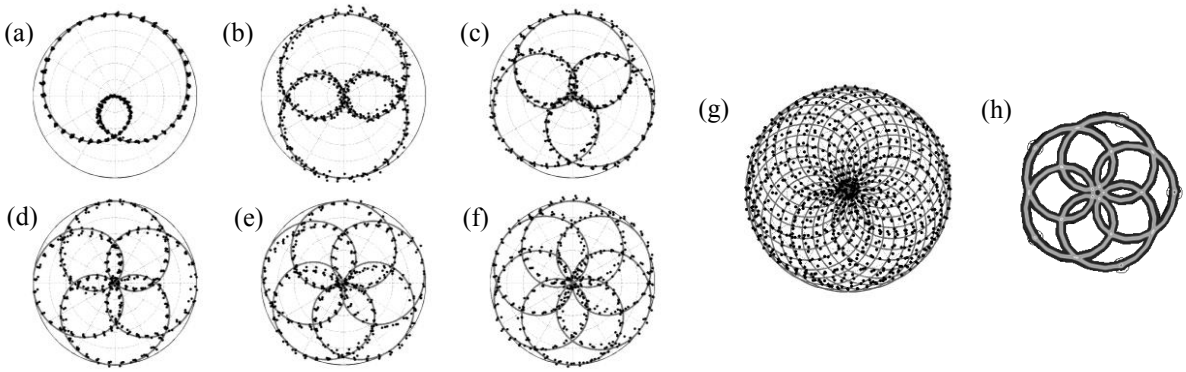

Fig. 3. Measurements (black dots) and calculations (grey curves) for modulation patterns at signal difference frequencies of (a) 1 GHz, (b) 2 GHz, (c) 3 GHz, (d) 4 GHz, (e) 5 GHz, (f) 6 GHz, (g) 6.25 GHz, and (h) 5 GHz with averaging. In all cases, the frequency of the LO laser was positioned 1 GHz from that of one of the signal lasers.

3. Measurement results

Plots (a) through (f) of Fig. 3 show measurements made by the OMA at signal laser difference frequencies between 1 and 6 GHz in 1 GHz increments. In each case the agreement between the measurement and calculation is very good and clearly indicates the expected correspondence between the number of lobes and the ratio of the frequency differences. Because of the fixed frequencies and minimal optical power drift, the modulation patterns were stable and required no adjustments, either during or between measurements. However, the measurements as shown were shifted slightly in the vertical and horizontal directions to center the patterns, and then rotated for angular alignment. Despite the phase-locks, the angular alignment was necessary because the signal and LO light was delivered to the OMA on separate optical fiber paths that were subject to thermal and mechanical drift between measurements.

Plot (g) of Fig. 3 demonstrates how easily a much more complicated pattern can be generated simply by using a non-integer difference frequency. In this example the difference frequency was 6.25 GHz, which requires four times as many lobes, or 25, in order for the pattern to repeat an integer number of times in the complex plane.

The measurements (a) through (g) capture only 10 to 20 ns snap-shots of the modulation and encompass at most a few complete rotations of the complex plane, thereby minimizing the impact of processing algorithms. By contrast, a long measurement can be used specifically to test the effectiveness of software processing and the stability of OMA hardware. Plot (h) of Fig. 3 shows a measurement of 5 μs in duration that relies on OMA software routines to clearly present a pattern with a 5 GHz difference frequency. This result was obtained with a 5-states APSK demodulation routine followed by an exponential RMS average, resulting in an error-vector magnitude below 3 %.

The stability of the signal itself is an important consideration. The 5 kHz linewidth of the LO laser corresponds to a stability of about 200 μs without phase-locking. However, with phase-locking the stability is extended to the range of seconds before being limited by the thermal and mechanical stability of the optical fibers.

4. Conclusion

We have demonstrated a family of calibration signals in the complex measurement plane that are easy to control, stable, and predictable from first principles. The modulation patterns can be made arbitrarily complicated based simply on the electrical control of the difference frequencies between the lasers. For calibration purposes, these patterns have the potential to be used for quantitative comparisons that would rigorously test characteristics such as amplitude and phase distortion, noise, and algorithm operation.

5. References

[1] P. A. Andrekson, "Metrology of complex optical modulation formats," Tech. Digest of the Optical Fiber Communications Conference, OWN1 (2010).
[2] C. Dorrer, D. C. Kilper, H. R. Stuart, G. Raybon, and M. G. Raymer, "Linear Optical Sampling," Photon. Tech. Lett. **15**, 1746 - 1748 (2003).
[3] P. A. Williams, T. Dennis, I. Coddington, W. C. Swann, and N. R. Newbury, "Vector signal characterization of high-speed optical components by use of linear optical sampling with milliradian resolution," Photon. Tech. Lett. **20**, 2007- 2009 (2008).
[4] M. Westlund, M. Skold, and P. A. Andrekson, "All-optical phase-sensitive waveform sampling at 40 GSymbol/s," Tech. Digest of the Optical Fiber Communications Conference, PDP12 (2008).
[5] T. S. Clement, P. D. Hale, D. F. Williams, J. C. M. Wang, A. Dienstfrey, and D. A. Keenan, "Calibration of sampling oscilloscopes with high-speed photodiodes," IEEE Trans. Microw. Theory Tech. **54**, 3173 - 3181 (2006).
[6] T. Dennis and P. D. Hale, "High-accuracy photoreceiver frequency response measurements at 1.55 μm by use of a heterodyne phase-locked loop," Opt. Express **19**, 20103 – 20114 (2011).